A COMPARISON OF TWO ACTIVE CONTROL METHODS THROUGH AN INVESTIGATION OF NODE STRUCTURES

John W. Parkins and Jiri Tichy

Graduate Program in Acoustics
The Pennsylvania State University
State College, PA 16804

Scott D. Sommerfeldt

Dept. of Physics & Astronomy
Brigham Young University
Provo, UT 84602

INTRODUCTION

In previous research, active control systems based on minimizing the sum of the squared pressures at discrete locations have been constructed for use in three-dimensional enclosures such as aircraft cabins.[1] More recently, a control system based on minimizing the sum of the energy densities at discrete points in space has been constructed, which was also targeted for use in aircraft cabins. The energy density based control system was tested under various control source/control sensor configurations in a rectangular room measuring 1.5 m $\times$ 2.4 m $\times$ 1.9 m, and compared to the results from measuring the performance of the squared pressure based method under the same conditions.[2] The results of these experiments has provided anecdotal information and a qualitative comparison between the two control methods, but a more quantitative comparison of the two control systems was desired. In this paper, a method of comparing the performance of the two control systems, based on analyzing the nodal surfaces of the squared pressure and total energy density fields, is investigated.

ACTIVE CONTROL STRATEGIES DEFINED

The active control method based on minimizing the sum of squared pressures minimizes the cost function

$$J_{SP} = \sum_{i=1}^{I} \left| \hat{p}(\boldsymbol{x}_i) \right|^2 , \tag{1}$$

where $\hat{p}(\boldsymbol{x}_i)$ is the complex pressure located at $\boldsymbol{x}_i$, and there are I sensors. The energy density based control system minimizes the cost function

$$J_{ED} = \sum_{i=1}^{I} \frac{1}{4\rho c^2} \left|\hat{p}(\boldsymbol{x}_i)\right|^2 + \frac{\rho}{4} \left|\hat{\boldsymbol{v}}(\boldsymbol{x}_i)\right|^2, \tag{2}$$

where $\hat{\boldsymbol{v}}(\boldsymbol{x}_i)$ is the vector particle velocity at $\boldsymbol{x}_i$, ρ is the density of air and c is the speed of sound. All three orthogonal components of the vector velocity are required, along with the pressure for an energy density measurement. Thus, a single energy density sensor requires four times the control processing as a single pressure sensor. (Research into the accuracy of a practical energy density sensor was recently conducted.[3]) Also of interest is the control strategy based on minimizing the total potential energy in an enclosure which minimizes the cost function

$$J_{PE} = \int_V \frac{1}{4\rho c^2} \left|\hat{p}(\boldsymbol{x})\right|^2 dV. \tag{3}$$

The total volume of the enclosure is V. The total potential energy based control method has been suggested as an optimal control system. Though it cannot be implemented physically this control method can be modeled and its performance used as a baseline.

SPATIAL DEPENDENCE OF ERROR SENSORS

For a given control source configuration, the modes individual sources are able to generate are the same for both squared pressure and total energy density control systems. Therefore, the pressure fields both control systems are capable of generating are also the same. On the other hand, the control systems differ in their ability to sense modes. If a sensor is located at a node, the control system does not observe this mode and controls the acoustic field regardless of the consequences to this mode. The control system can actually amplify the energy of the mode, causing the total potential energy in the enclosure to increase; this is sometimes referred to as "control spillover." It is therefore critical for sensors to be located away from nodes. The total potential energy can also be increased due to a control system if the sensor is located in regions of low acoustic field strength. This occurs when all of the modes generally destructively interfere in a region. Hence, the performance of a control system varies as the sensor is at different locations in an enclosure. The sensor might be located at nodes for some modes as well as regions of overall low field strength, which generally yields poor cancellation performance. Other times, the sensor might be located at positions which yield substantial cancellation performance.

In Fig. 1, the simulated reduction in total potential energy in an enclosure measuring 1.5 m × 2.4 m × 1.9 m is plotted versus frequency for the integrated potential energy density control method. As mentioned earlier, the integrated potential energy density control results are used as a baseline for comparing other active control methods. The data were generated using a model consistent with an experimental enclosure used for active control experiments. One control source and one noise source were used for this configuration. For this optimal control method, the total potential energy in the enclosure can never be increased, by definition. Reduction in the total potential energy tends to occur at resonance frequencies. Slight changes in the excitation frequency near resonance can be seen to have a significant effect on the cancellation

Using the same noise and control source configuration, a single sensor was placed in ten discrete locations within the enclosure for ten control simulations. These ten locations were equally spaced along a diagonal line originating at the normalized point (0, 0, .20) and ending at the normalized point (1, .80, .60). In Fig. 2 and Fig. 3, ten plots are overlaid of the total potential energy reduction versus frequency for each sensor location for the squared pressure and total energy density control, respectively. From Fig. 2 and Fig. 3, it can be seen that the performance of the total energy density control is much less dependent on error sensor location compared to that of squared pressure control. Also, when the squared pressure control increases the total potential energy at some frequencies, it produces much greater amplifications

than the total energy density control. Though these data are anecdotal in nature, it demonstrates the relative dependence of the two control methods on sensor location. It will be shown in the following sections that the total energy density field varies less, spatially, than the squared pressure field, which explains why the total energy density control method is less sensitive to error sensor location.

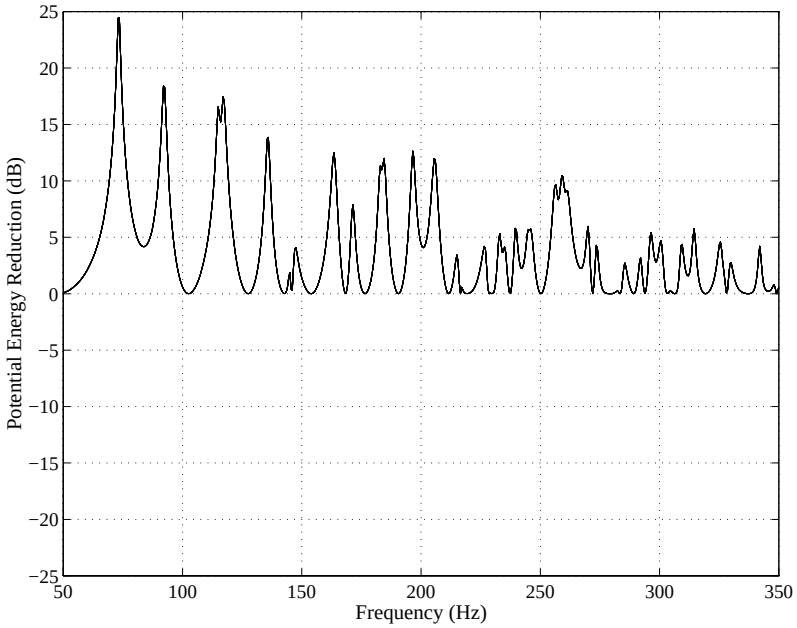

Figure 1. Predicted integrated potential energy control for a noise source at (.12, .97, .97) and a control source at (.05, .11, .04).

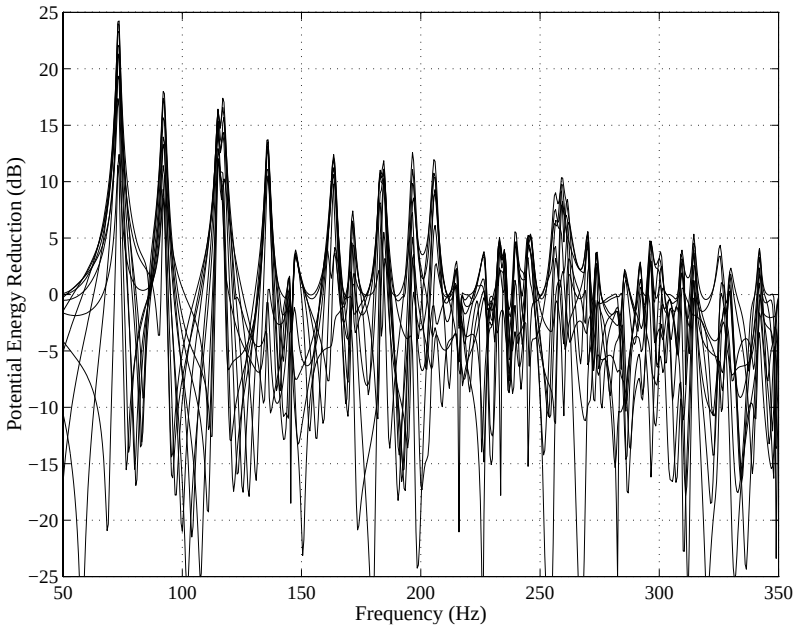

Figure 2. Predicted squared pressure control for a noise source at (.12, .97, .97), a control source at (.05, .11, .04) and one error sensor. The error sensor is placed at ten different locations yielding ten cancellation curves.

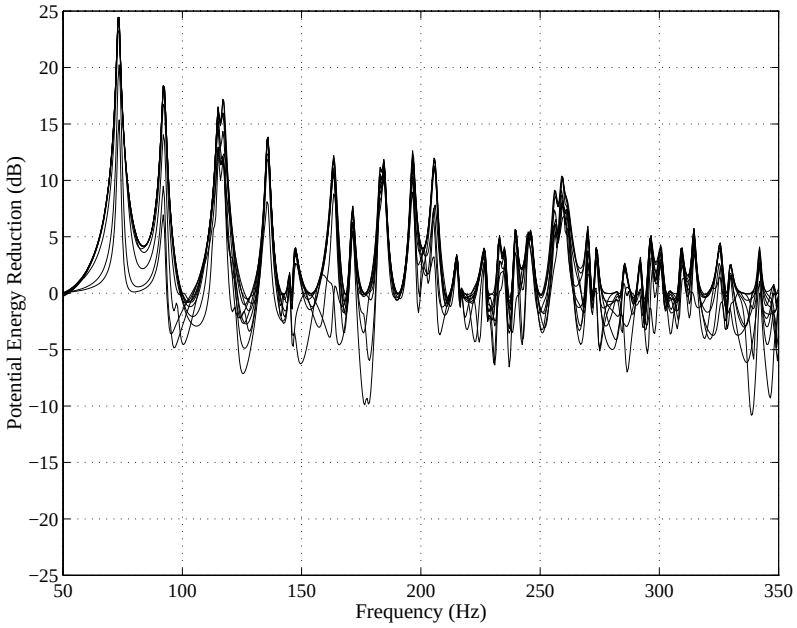

Figure 3. Predicted total energy density control for a noise source at (.12, .97, .97), a control source at (.05, .11, .04) and one error sensor. The error sensor is placed at ten different locations yielding ten cancellation curves.

SQUARED PRESSURE AND TOTAL ENERGY DENSITY FIELD NODAL VOLUMES

The normalized squared pressure and normalized total energy density fields for the (*l*, *m*, *n*) mode are described by

$$p_n^2(\mathbf{x}) = \cos^2 k_x x \cos^2 k_y y \cos^2 k_z z \tag{4}$$

$$e_n(\mathbf{x}) = \frac{1}{k^2}\left(k_x^2 \cos^2 k_y y \cos^2 k_z z + k_y^2 \cos^2 k_x x \cos^2 k_z z + k_z^2 \cos^2 k_x x \cos^2 k_y y\right) \tag{5}$$

where $k_x = l\pi / L_x$, $k_y = m\pi / L_y$ and $k_z = n\pi / L_z$.

The locations of the nodes of these fields are determined by setting Eqs. (4) and (5) to zero. Therefore, the squared pressure field has nodes where $\cos k_x x$, $\cos k_y y$ or $\cos k_z z$ are zero. These nodes are located at

$$
\begin{aligned}
x &= \frac{\pi}{k_x}\left(\frac{2i+1}{2}\right), \quad 0 \le x \le L_x, \quad i = 0,1,2\text{K} \\
y &= \frac{\pi}{k_y}\left(\frac{2j+1}{2}\right), \quad 0 \le y \le L_y, \quad j = 0,1,2\text{K} \\
z &= \frac{\pi}{k_z}\left(\frac{2k+1}{2}\right), \quad 0 \le z \le L_z, \quad k = 0,1,2\text{K}
\end{aligned} \tag{6}
$$

which define nodal planes. There are *l* nodal planes perpendicular to the *x*-axis, *m* nodal planes perpendicular to the *y*-axis and *n* nodal planes perpendicular to the *z*-axis for an (*l*, *m*, *n*) mode. Nodes for the total energy density field, on the other hand, exist only when all three terms of Eq. (5) are zero. This only occurs where the nodal planes of the squared pressure field intersect. Thus, the nodes of the total energy density field exist as lines.

If only one mode were present in an acoustic field, a control system would attenuate the total potential energy if the control source(s) were capable of producing the mode and the sensor(s) were not located exactly on a node. In practice, multiple modes always contribute to the field. In this case, the sensor(s) need to be located far enough away from a node so that the dominant mode in the field has the highest contribution for at least one sensor location. There are therefore, regions that are volumes where locating the sensor(s) yields poor control performance. These regions will be referred to as nodal volumes. The size of these nodal volumes can be compared to gauge the performance of the squared pressure control compared to the total energy density. The nodal volume is a function of the contribution of the secondary modes, which is a function of the damping and modal density of the enclosure.

The squared pressure field and total energy density field nodal volumes are defined by the regions where $p_n^2(\mathbf{x}) < \varepsilon$ and $e_n(\mathbf{x}) < \varepsilon$ for a given mode. For a given ε, all oblique modes yield the same total nodal volume. This is true for tangential and axial modes as well. Examples of nodal volumes for the (1, 1, 0) mode are depicted in Fig. 4. Fig. 4 shows contour plots of the total energy density and squared pressure fields. Since there is no dependence of the fields on *z*, the nodal volumes are the regions within a given contour extruded in the *z*-direction. The nodal volumes for the total energy density field are much smaller than those of the squared pressure field. As ε is increased the nodal volumes of the squared pressure and total energy density fields become closer in size.

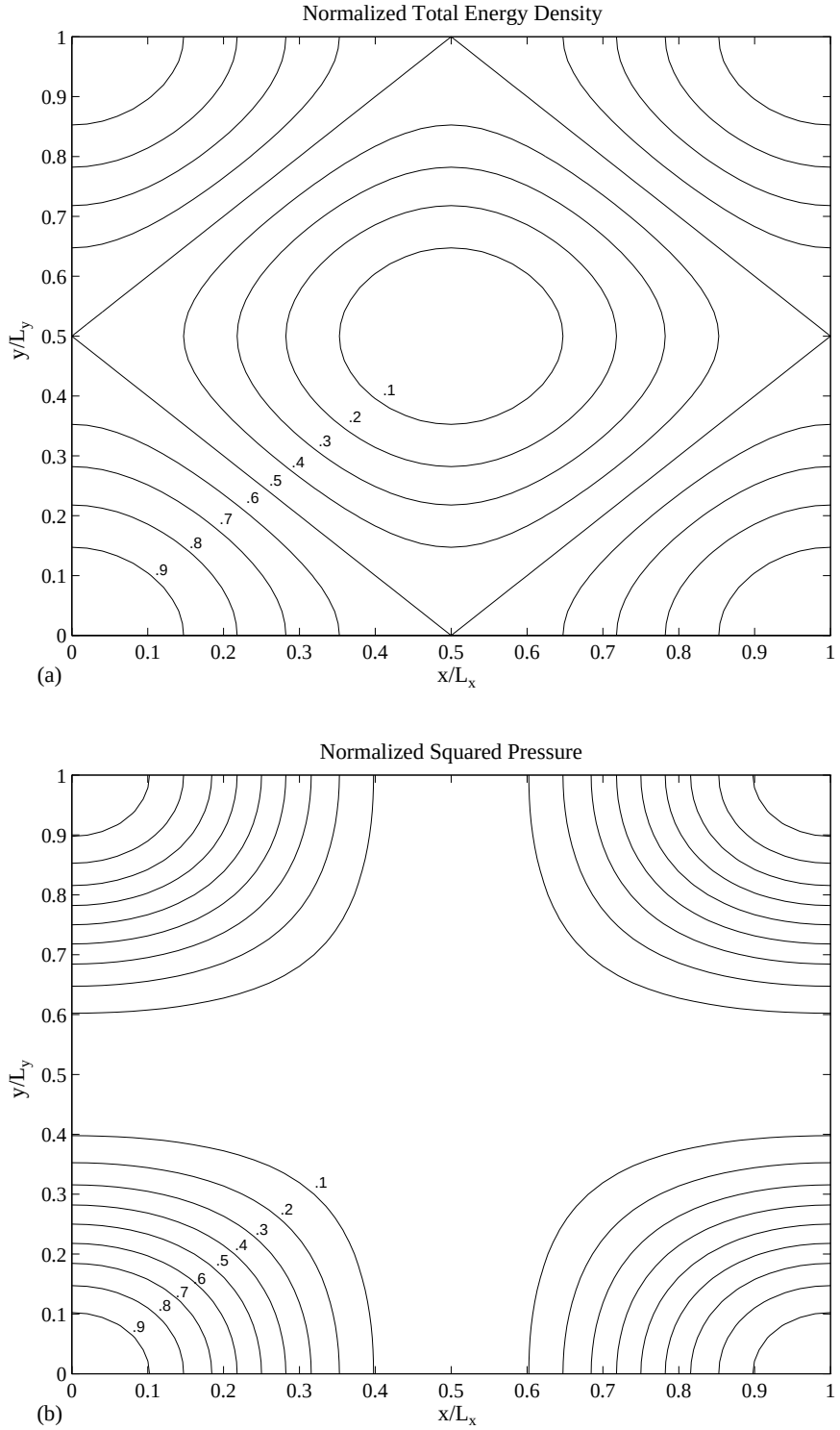

Figure 4. Normalized (a) total energy density field and (b) squared pressure field contour plots for mode (1, 1,0).

SINGLE SENSOR PROBABILITY COMPARISONS

The probability that a randomly placed sensor is located in a nodal volume can be expressed as

$$P = \frac{V_{node}}{V} \tag{7}$$

where V_{node} is the total nodal volume, and V is the total volume of the enclosure. The squared pressure and total energy density control methods can be compared by calculating the probabilities of a randomly placed sensor lying in axial, tangential and oblique nodal volumes. When k_x, k_y and k_z are all non-zero, Eqs. (4) and (5) represent the fields for the oblique modes. Tangential mode equations are found by setting only one axial wavenumber k_i to zero. An example of tangential mode equations is given by

$$p_n^2(\mathbf{x}) = \cos^2 k_x x \cos^2 k_y y \tag{8}$$

and

$$e_n(\mathbf{x}) = \frac{1}{k^2}\left(k_x^2 \cos^2 k_y y + k_y^2 \cos^2 k_x x\right), \tag{9}$$

where for this case $k_z = 0$. Axial mode equations are found by setting two axial wavenumbers to zero. Example equations for axial modes are given by

$$p_n^2(\mathbf{x}) = \cos^2 k_x x \tag{10}$$

and

$$e_n(\mathbf{x}) = 1 \quad , \tag{11}$$

where in this case k_y and k_z are set to zero. For the total energy density axial mode, the field has no spatial dependence, and there are no nodes. Therefore, an energy density sensor could be placed anywhere in a one-dimensional field without the possibility of lying on an axial mode node. This is particularly relevant in controlling fields in ducts. The energy density field nodal volumes are smaller than those of the squared pressure field for all mode types.

The probabilities of a randomly placed single sensor lying on a nodal volume versus ε for both the squared pressure and total energy density fields are plotted in Fig. 5. These plots were generated numerically. The three-dimensional squared pressure and total energy density fields for an axial, tangential and oblique mode were first discretized. The regions where the magnitude of the fields were less than ε were summed and divided by the total volume of the enclosure, to yield the probability.

The probability for the axial mode of the total energy density field is independent of ε and is identically zero. The probability of a randomly placed single sensor lying in a nodal volume for the total energy density field is always less than that of the squared pressure field. This is consistent with the results shown in Fig. 2 and Fig. 3. The results in Fig. 5 indicate the superior performance of total energy density control when a single sensor is used.

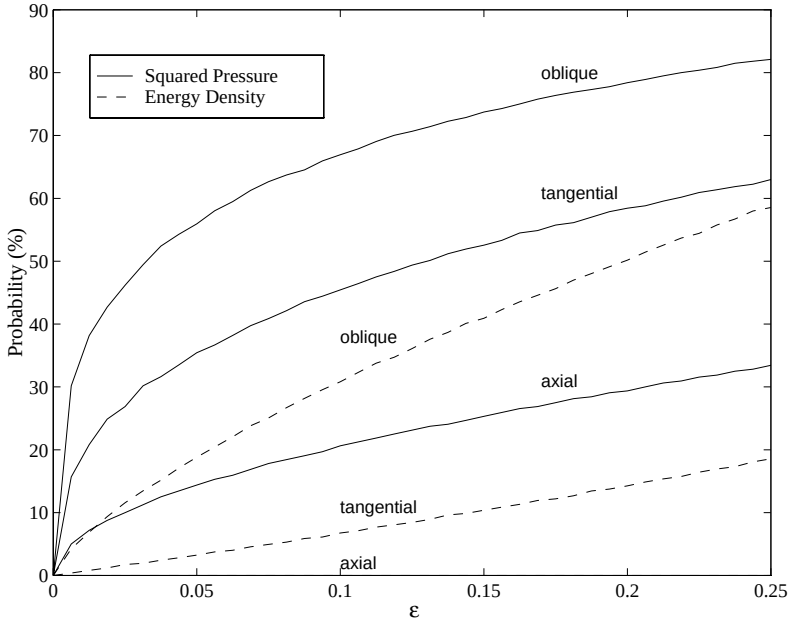

Figure 5. Probability of a randomly placed error sensor being located in a nodal volume for the axial, tangential, and oblique modes.

MULTIPLE SENSOR PROBABILITY COMPARISONS

So far, the performance of the total energy density and squared pressure control methods have been compared when one sensor is used. As the number of error sensors is increased, the chances that all the sensors are located in a nodal volume decreases substantially. In this section, the number of microphones necessary for the squared pressure control to equal or surpass the performance of a single sensor for total energy density control is investigated.

The probability of n randomly placed sensors all lying in nodal volumes is $P_n = P^n$. The squared pressure curves of Fig. 5 can be raised to the n^{th} power to determine the number of pressure sensors necessary to equal the performance of one energy density sensor. Figs. 6, 7 and 8 show the probability of n randomly placed pressure sensors lying in a nodal volume versus one energy density sensor for the axial, tangential and oblique modes, respectively. In Fig. 6 the total energy density field has no nodal volumes, so the probability of a single energy density sensor lying in a nodal volume is zero and always less than the probability of n pressure sensors all lying in a nodal volume. On the other hand, in Fig. 7 four or more pressure sensors yield a lower probability than a single energy density sensor, while in Fig. 8 three pressure sensors slightly outperform a single energy density sensor for the oblique modes. The worst case comparison of the total energy density sensor to the pressure sensor occurs for a field composed of only oblique modes. Approximately three pressure sensors would be required for every one energy density sensor for the squared pressure control system to match the performance of the total energy density control system.

However, in practice the pressure fields are composed of all three types of modes. It is more important to be able to control axial modes over tangential modes since the axial modes have higher total

potential energy than the other two modes. The relative total potential energies of the axial, tangential and oblique modes are $\frac{1}{2}$, $\frac{1}{4}$ and $\frac{1}{8}$.[4]

The number of axial modes whose frequencies are less than a given frequency f is

$$N_{axial} = \frac{Lf}{8c}, \tag{12}$$

where $L = 4\left(L_x + L_y + L_z\right)$.[5] For tangential modes,

$$N_{tang} = \frac{\pi}{4} S\left(\frac{f}{c}\right)^2 \tag{13}$$

and for oblique modes

$$N_{oblique} = \frac{4\pi}{3} V\left(\frac{f}{c}\right)^3, \tag{14}$$

where $S = 2\left(L_x L_y + L_x L_z + L_y L_z\right)$ and $V = L_x L_y L_z$. At lower frequencies then, the ratio of tangential modes to oblique modes increases. Since the performance of the total energy density method improves relative to the squared pressure control method for tangential and axial modes, the performance of the total energy density system improves relative to the squared pressure control system at lower frequency.

From the statistical data presented in this paper, it is expected that at least three pressure sensors would be necessary to match the performance of one energy density sensor in a field made up of many modes, but it is unknown exactly how many more sensors would be required. From observation of the statistical data, possibly four times as many pressure sensors as energy density sensors would be necessary for the squared pressure control system to match the performance of the total energy density control system. To test this hypothesis, the performance of three and four pressure sensors were compared to the performance of one energy density sensor in simulations. The results of the simulations are shown in Fig. 9 and Fig. 10. The cancellation performance of integrated potential energy density, squared pressure and total energy density control are compared when two control sources are used. Fig. 9 shows the results of using three pressure sensors to one energy density sensor, while Fig. 10 shows the results of four pressure sensors to one energy density sensor. Though the data are anecdotal, these examples indicate that no more than four pressure sensors might be needed to match the performance of one energy density sensor for fields composed of many types of modes.

CONCLUSIONS

Multiple pressure sensors are needed for the squared pressure control method to match the performance of a single energy density sensor for the total energy density control. But the current control algorithm for the total energy density control method requires four processing channels for each energy density sensor. Each energy density sensor must provide the pressure and the three orthogonal components of particle velocity at its location. The minimum number of microphones needed to measure the total energy density is four (in a tetrahedral configuration), though six were used in this research. For the sensor employing a tetrahedral configuration, calculation of the particle velocities is more involved. The particle velocities for either sensor must be determined either digitally or by analog circuits. The computational power needed for comparable squared pressure and total energy density systems is therefore slightly higher for the total energy density control method. Two advantages are recognized for the total energy density control method though. First, compact energy density sensors can be used whereas approximately four times the number of pressure sensors must be randomly distributed in space for the squared pressure

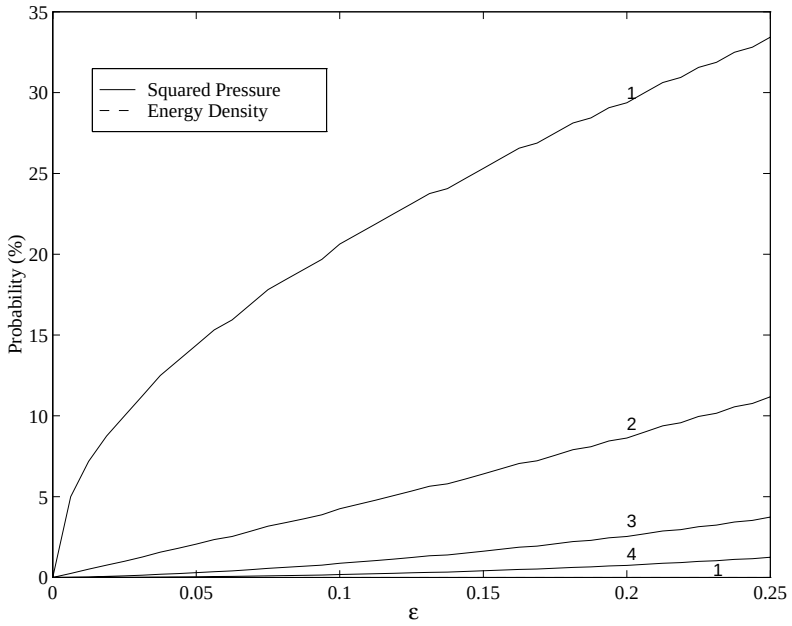

Figure 6. Probability of *n* randomly placed error sensors all being located in a nodal volume for the axial modes.

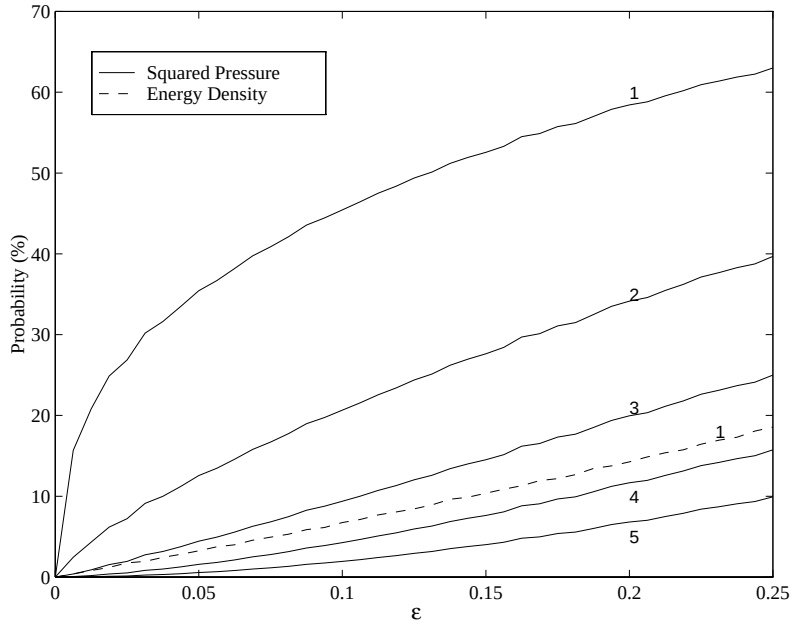

Figure 7. Probability of *n* randomly placed error sensors all being located in a nodal volume for the tangential modes.

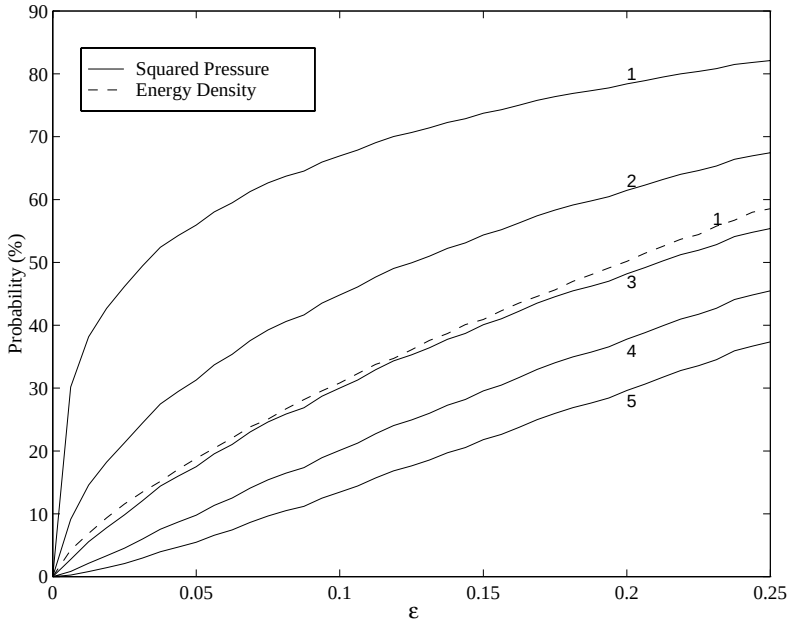

Figure 8. Probability of *n* randomly placed error sensors all being located in a nodal volume for the oblique modes.

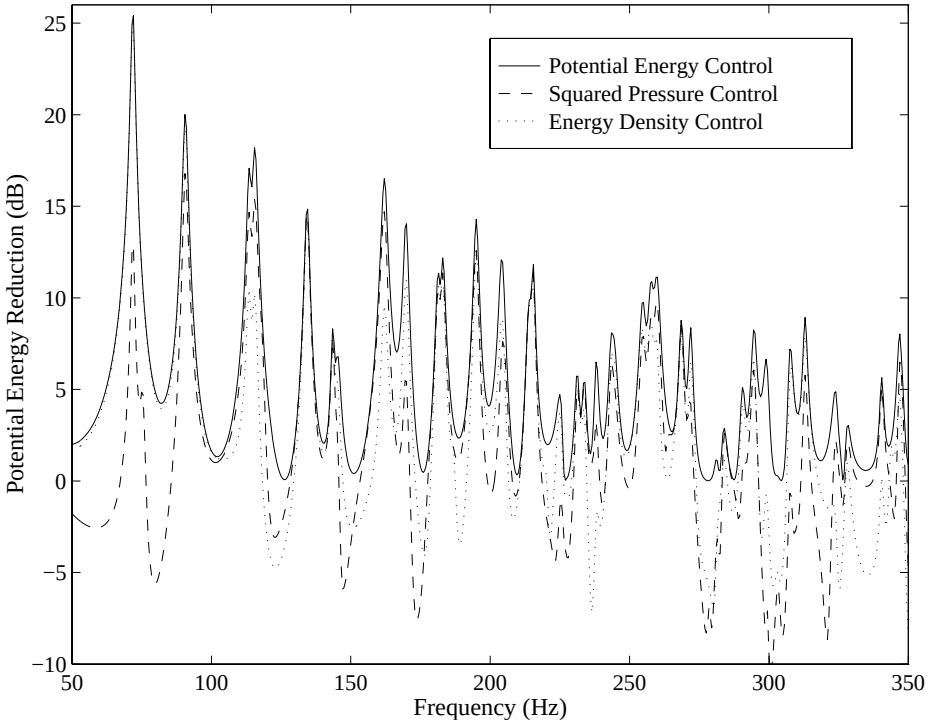

Figure 9. Predicted control for integrated potential energy density, squared pressure and total energy density control methods. Two sources at (.05, .11, .04) and (.34, .96, .04). Three pressure sensors at (.68, .40, .48), (.34, .67, .24) and (.14, .15, .71). One energy density sensor at (.68, .40, .48).

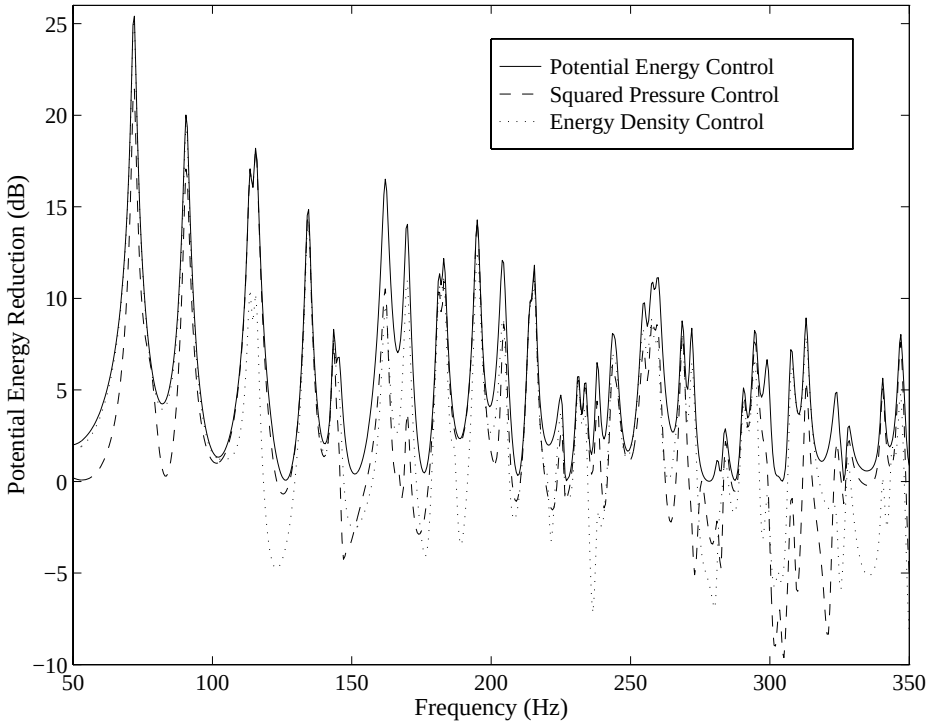

Figure 10. Predicted control for integrated potential energy density, squared pressure and total energy density control methods. Two sources at (.05, .11, .04) and (.34, .96, .04). Four pressure sensors at (.68, .40, .48), (.34, .67, .24), (.14, .15, .71), and (.14, .75, .43). One energy density sensor at (.68, .40, .48).

control method. Sometimes it is undesirable to have to locate so many sensors and to provide the necessary cabling in installations such as aircraft cabins. Also, the performance of the total energy density control system improves at lower frequencies relative to the squared pressure control system. For low-frequency applications, the total energy density system might be the more appropriate active control solution. In addition, one could potentially modify the control algorithm so that only a single signal from the energy density sensor is needed. Although use of a single energy density signal was not investigated in this work, this approach has the potential to overcome the disadvantage of increased computational complexity.

REFERENCES

1. "In-flight experiments on the active control of propeller-induced cabin noise," S. J. Elliot, P. A. Nelson, I. M. Stothers and C. C. Boucher, *J. Sound and Vib*., **140**, 219-238, (1990).
2. "Narrowband and broadband active control in an enclosure using the acoustic energy density," J. W. Parkins, S. D. Sommerfeldt, and J. Tichy, *Submitted for publication to J. Acoust. Soc. Am*., 1999.
3. "Error analysis of a practical energy density sensor," J. W. Parkins, S. D. Sommerfeldt, and J. Tichy, *Submitted for publication to J. Acoust. Soc. Am*., 1999.
4. P. M. Morse, *Vibration and Sound*, (Acoustical Society of America, New York, 1976).
5. H. Kuttruff, *Room Acoustics, Third Edition*, (Elsevier Applied Science, New York, 1991).